Cyclone Tracking in Different Spatial and Temporal Resolutions

R. BLENDER AND M. SCHUBERT

Meteorologisches Institut, Universität Hamburg, Hamburg, Germany

ABSTRACT

The quality of cyclone tracks associated with model output of various resolutions is determined using a high-resolution dataset ($1.125° \times 1.125°$, 2 h) mapped to different spatial (triangular truncations, T21, T42, T63, T84) and temporal resolutions (4 h, 6 h, 12 h, 18 h, 24 h). Three sets of comparisons are performed to study the impact of increasing (i) temporal, (ii) spatial, and (iii) spatiotemporal resolutions (T21/24 h, T42/12 h, T63/6 h, T84/4 h). The different "test" resolutions are compared with a "perfect" reference dataset of optimal resolution. A general method to quantitatively compare two sets of tracks is developed. For a given test dataset, this method yields the ratio of perfect tracks (which are also identified in the reference set) and the ratio of missing tracks (present in the reference set, but missing in the test set). In 24-h data (T42) only about 45% of the cyclones can be identified with cyclones in 2-h data (73% in 12 h, 85% in 6 h).

1. Introduction

Automatic tracking of cyclones has become a common tool in meteorological data analysis (Alpert et al. 1990; Murray and Simmonds 1991; Haak 1993; König et al. 1993; Ueno 1993; Hodges 1994; Blender et al. 1997; Sinclair 1997; Schubert et al. 1998; Sickmöller et al. 2000). Cyclone tracks yield the locations of storms and precipitation, and modifications of the mean tracks, caused either by anthropogenic causes or by a long-term natural variability, have strong influences on regional climates. The use of numerical tracking algorithms is necessary because of the large amount of data and the need for the objective detection of changes in climate studies. Tracking algorithms are able to identify tracks of other meteorological objects as well, like clouds or water vapor anomalies, which yield information on the transport by wind fields. Although the methods and the results presented here pertain to any kind of extrema in fields, cyclones are used throughout.

Our experience revealed the enormous dependence of cyclone tracks on the quality of the datasets (Schubert 1996; Wilshusen 1996). There is considerable difference between tracks identified in high resolution, for example, T106 ($1.125° \times 1.125°$), 6-hourly separated data, and in low-resolution data, for example, T21 ($5.625° \times 5.625°$), with a 24-h time spacing. The tracking is difficult in high spatial resolutions since the number of

cyclones is high, and in low temporal resolutions because the search areas that have to be scanned are large. These problems may be less relevant in subjective analyses (e.g., Klein 1957) where the manifold meteorological knowledge on the dynamics allows one to identify cyclones and their tracks also in data with high temporal intervals. This knowledge is typically not available to automatic routines. Clearly, the tracks depend on the tracking method (Sinclair 1997) and on the meteorological fields used, for example, the pressure or the vorticity.

The aim of the present paper is to investigate objectively the quality of cyclone tracks in data with a variety of spatial and temporal resolutions. The result is a guideline to estimate the number of correct and missing tracks in a given dataset. The basis is a high-resolution (T106, 2 h) dataset that is mapped on coarser resolutions. The tracks are extracted using a nearest-neighbor search method applied in previous studies (Blender et al. 1997, henceforth referred to as BFL; Schubert et al. 1998). The quality of tracks in the given "test" dataset is obtained by the comparison with a high-resolution "reference" dataset, which is assumed to produce perfect tracks. The comparison between the two sets of tracks is performed by the identification of associated pairs of tracks in the sets using a distance measure for tracks (mathematically a metric that considers spatial as well as temporal distances of curves). The number of these pairs yields an objective measure for the overlap of both sets, and hence a measure for the quality of the tracks in the given (test) data. Subjectively determined tracks are not included in this study because these data depend on the particular human experience. A climatological

Corresponding author address: Dr. Richard Blender, Meteorologisches Institut, Universität Hamburg, Bundesstr. 55, D-20146 Hamburg, Germany.
E-mail: blender@dkrz.de

TABLE 1. Number N_g of zonal grid points and resolution $\Delta\phi$ (in degrees) for different triangular wavenumber truncations.

	T21	T42	T63	T84	T106
N_g	64	128	192	256	320
$\Delta\phi$	5.625	2.812	1.875	1.406	1.125

approach is not pursued because too much statistical information is necessary to cover the information given by the individual tracks.

In section 2 the dataset and in section 3 the cyclone tracking algorithms are described. Section 4 contains the derivation of the method to compare two sets of tracks. In section 5 the results for several comparisons are presented. The results are summarized in section 6 and discussed in section 7.

2. Data

The data basis is the output of a simulation with the Hamburg climate model ECHAM4, using the Atmospheric Model Intercomparison Project SST between October 1992 and March 1993 (Roeckner et al. 1996). The spatial resolution of the data is given by the triangular wavenumber truncation T106, and the time interval is 2 h. To determine the cyclone positions, the 1000-hPa geopotential height (z1000) is used. The analysis is global and restricted to the winter season (December, January, and February). The data are mapped to different lower spatial resolutions shown in Table 1, where N_g is the number of zonal grid points (the number of meridional grid points is $N_g/2$) and $\Delta\phi$ is the resolution in degrees. Data for the low-resolution grids are linearly interpolated.

3. Cyclone track search

The cyclone positions are defined by local minima of the geopotential height (z1000) of the 1000-hPa surface considering the neighborhood of eight grid points. Additionally, in order to locate intense vortices, a minimum value g_{min} for the mean gradient of z1000 in a synoptic neighborhood is required. The threshold used in this study is $g_{min} = 100$ m $(1000\ km)^{-1}$, which corresponds to roughly 12 hPa $(1000\ km)^{-1}$ This value restricts the analysis to intense extratropical storms. The minimum lifetime of the cyclones is 3 days. The tracking method used has been applied in studies of observed cyclone tracks (BFL) and in the analysis of a scenario experiment (Schubert et al. 1998).

Tracks are constructed by a nearest-neighbor search in the preceding data field around a cyclone position. The search range extends up to a width, which corresponds to a speed of roughly 100 km h^{-1} in 6 h. However, midlatitude cyclones show a nonlinear growth of the mean square displacement of (BFL)

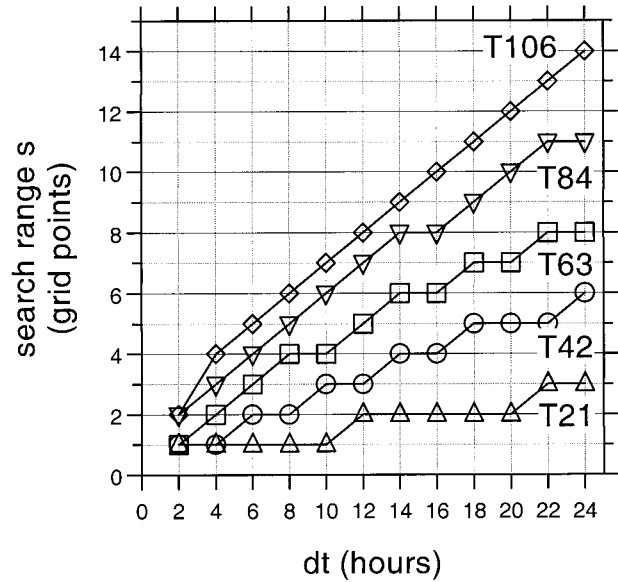$$\langle r^2 \rangle \sim t^k \qquad (1)$$

FIG. 1. Search range (at the equator) according to Eq. (2) vs time step for different spatial resolutions (wavenumber truncations) as indicated.

with an observed exponent $k \approx 1.5$. Therefore, it is assumed that the search range s in zonal grid points grows with the time interval $dt^{1.5/2}$

$$s = \frac{N_g}{64} \frac{(dt/dt_0)^q}{\cos\phi}, \quad \text{(rounded)}, \qquad q = 0.75, \quad (2)$$

where $dt_0 = 6$ h and N_g is the number of zonal grid points. The rounded whole value of s is used, and a minimum value $s = 1$ is required. The zonal search range (in grid units) increases poleward with the latitude ϕ to account for the decreasing longitudinal distance of grid points. Figure 1 shows the search range at the equator for the different spatial resolutions. In T21 ($N_g = 64$) and $dt = 6$ h, (2) yields $s = 1$ at the equator, whereas for $dt = 24$ h, the range reaches only $s = 3$, and not $s = 4$ as in a linear growth.

The growth (2) of the search range is lower than linear and has therefore an important and useful impact on the tracking. A major problem in the tracking is caused by the number of cyclones within the search region; the larger this number, the more difficult it is to connect the cyclones to correct tracks. This number is proportional to the density of cyclones and to the search area, which grows according to $(dt)^{1.5}$ here. In a linear growth formula, the search area would be larger, proportional to $(dt)^2$, and the attribution would be more difficult.

The search range extends s grid points eastward and westward ($2s + 1$ points for the total width). In the meridional direction, the search range is smaller, $(2s + 1)/2$, that is, slightly more than half of the zonal range. However, an increase of the meridional search range up to the zonal range does not alter the results for the tracks. The search is applied backward in time, scanning the

search area around the cyclones. The search starts with zero shell width, which increases for all cyclones simultaneously until the search range s is reached. Therefore, the nearest cyclone in the preceeding field is attributed, and stationary cyclones are detected first. The results of the algorithm are in agreement with those of a subjective analysis (Schubert 1996; Wilshusen 1996).

4. Track comparison method

In the present study, two sets of tracks obtained by the search algorithm in the section above have to be compared. One set is the reference set with tracks determined in the data with optimal resolution (e.g., $dt = 2$ h), and the other set is a test set. Since the reference set is assumed to be perfect, the agreement between both sets is a measure of the quality of the tracks in the test set. The approach is Lagrangian and compares individual tracks, whereas an Eulerian approach would compare densities of tracks and other derived fields. The Lagrangian approach is chosen because it is difficult to capture the complete Lagrangian track information by an Eulerian statistic. Furthermore, the number of cyclones within one winter season is too low to determine a conventional Eulerian cyclone climatology. The sets correspond to either different spatial and temporal resolutions, or both. The task faces several problems: (i) the numbers of tracks may be different in the two sets, (ii) the individual tracks are defined on grids of different spacings, and (iii) the cyclones may occur at nonoverlapping time steps. In the following, an objective way to measure the agreement of two sets of tracks is presented. First, a method to measure the distance between two individual tracks out of two sets is derived. Based on this, the two sets are compared and the degree of correspondence is quantified.

a. Distance of two tracks

A distance (mathematically a metric) for two tracks is required, which, in general, are detected on different grids and time steps, and also may start and end at different times. There is even no need for a temporal overlap of the two tracks.

A track is defined as a sequence $\{x(a), y(a), t(a)\}$ of positions x, y and times t with the age $a = 0, \ldots, A$, A being the total lifetime. The time-dependent positions $\{\hat{x}(t), \hat{y}(t)\}$ are determined by the cyclone tracking algorithm and are related to this sequence by $\{\hat{x}[t(a)] = x(a), \hat{y}[t(a)] = y(a)\}$. A second track will be denoted by primed quantities, $\{x'(a'), y'(a'), t'(a')\}$, and $a' = 0, \ldots, A'$ with the lifetime A'. In the calculation, continuous values for the tracks are assumed, the extension to discrete time steps used in the analysis is straightforward.

The variance spanned by the two tracks is given by

$$\sigma_{12}^2 = \frac{1}{AA'} \int_0^A da \int_0^{A'} da'$$
$$\times \{\alpha([x(a) - x'(a')]^2 + [y(a) - y'(a')]^2)$$
$$+ \beta[t(a) - t'(a')]^2\}. \tag{3}$$

The factors α and β determine the weights of spatial and temporal distances. To obtain physically equivalent weights, typical values for the distance Δx and the time-scale Δt, are introduced, and a balance between the two sums in (3) is assumed

$$\alpha \Delta x^2 = \beta \Delta t^2. \tag{4}$$

Based on a typical speed, $U = \Delta x/\Delta t$, the ratio is

$$U^2 = \beta/\alpha. \tag{5}$$

The numerical calculations use the synoptic velocity scale, $U = 10$ m s^{-1}, and $\alpha = 1$.

The variance σ_{12}^2 is not yet suited as a measure for a distance because σ_{12} does not vanish for identical tracks, $\sigma_{11} \neq 0$. Hence, the distance D_{12} is defined

$$D_{12}^2 = \frac{1}{AA'} \left[\sigma_{12}^2 - \frac{1}{2}(\sigma_{11}^2 + \sigma_{22}^2) \right], \tag{6}$$

where the "self-variances," σ_{11}^2 and σ_{22}^2, are subtracted. This distance fulfills the conditions for a metric: it is positive for any different pair, and it vanishes for identical tracks. The mean age $\sqrt{AA'}$ is introduced in D_{12} because it is desirable that D_{12} decreases with increasing total length (age), if a constant deviation between the two tracks is present. Thus, a deviation between long tracks is less relevant in D_{12} than the same deviation between shorter tracks.

The spatiotemporal distance D_{12} is an objective measure of the deviation of two tracks, and it is applicable in situations with different grids and different observation times. Not only spatial discrepancies contribute to D_{12}, but also different genesis or lysis times of the two cyclone observations. If the same meteorological cyclone is identified in datasets with two different grids, there is a (small) contribution to D_{12} because the deviations of the grid points constrain the tracks to different positions (the same argument pertains to different observation times).

b. Agreement between two sets

To measure the agreement between two sets of tracks, corresponding tracks are identified using the distance D_{12} (6) between two individual tracks. The tracks in the reference set 1 are counted by $i_1 = 1, \ldots, N_1$ with the total number N_1, and the tracks in the test set 2 by $i_2 = 1, \ldots, N_2$ with the total number N_2. First, set 1 is scanned and for every i_1 the track i_2 in set 2 is searched with the minimum distance. This yields a table $i_2 = I_2(i_1)$, which contains the tracks of the next neighbors i_2 of every i_1.

Then, vice versa, set 2 is scanned and the nearest neighbor tracks i_1 in set 1 are searched. Thus, the table $I_1(i_2)$ is obtained, defining the tracks in the first set with a minimum distance to the tracks i_2 in the second set. Note that there is no need for these two tables to be the inverse of each other, simply because the numbers of tracks N_1 and N_2 are not necessarily equal.

These two comparisons allow one to identify those pairs of tracks that form one-to-one pairs (i_1, i_2), satisfying $i_1 = I_1 [I_2(i_1)]$, or equivalently $i_2 = I_2 [I_1(i_2)]$. These pairs consist of tracks that form unique neighbors in both sets. The number N_p of these pairs is a measure for the overlap of the two sets. From a meteorological point of view, this method identifies the two tracks in the two datasets that correspond to the same cyclone. The remaining tracks have neighbors in the other set, which are paired with different tracks. Clearly, the number N_p of pairs is restricted by the minimum of N_1 and N_2. The absolute value of the distance D_{12} of a pair is not relevant, but pairs identified in this way have typically low distances, and the study showed that the introduction of a reasonable upper limit does not alter the result significantly. Therefore, the method has the advantage that it is free of tunable parameters. In the comparisons, the first set is the *reference set* determined in an optimal resolution, for example, with the smallest time step *dt*. The second set is the *test set* with tracks obtained in a lower resolution.

If tracks in a given dataset (the test set) with a particular resolution are determined, the following questions arise:

1) How many of the detected cyclones in the test set agree with a (correct) track in the reference set?
2) How many of the (correct) cyclones in the reference set are not detected in the test set?

Based on the result given by the numbers N_1, N_2, and N_p, two normalized parameters are derived.

The first parameter gives the answer to the first question: p_a is the *probability of coincidence* for a track in the test set to agree with a track obtained in the (perfect) reference set. The probability p_a is given by the ratio of the number N_p of pairs and the number N_2 of tracks in set 2:

$$p_a = N_p/N_2. \quad (7)$$

This probability p_a is between $p_a = 0$, if all test tracks are completely wrong, and $p_a = 1$ if all test tracks can be identified with a perfect track. Therefore, p_a is a measure for the quality of the identified tracks.

The second question is answered by the second parameter, the ratio of tracks that are not identified in the test set, but are present in the reference set

$$r_m = \frac{N_1 - N_p}{N_2}, \quad (8)$$

where r_m is the ratio of missing tracks (compared to N_2).

For example, $r_m = 0$ denotes that no perfect track is missing in the test set. Any value $r_m > 0$ means that perfect tracks are not present in the test set. There is no upper limit for r_m. The second parameter r_m is necessary, because for a small number N_2 of tracks in the test set ($N_2 \ll N_1$), all of these could be identified with a perfect track ($p_a = 1$), but a large portion of reference tracks could be absent.

c. Sources of deviation

Several problems arise when two sets of tracks in different resolutions are compared (this pertains to any tracking method). These error sources can lead to a severe underestimation of the number of reliable tracks.

1) *Equality of numbers:* Clearly, the numbers of tracks in the sets should be approximately equal in order to obtain a satisfactory agreement. Unfortunately, this is not necessarily true if extremely different temporal or spatial resolutions are involved. In general, high spatial resolutions and low temporal resolutions yield high numbers of cyclones.
2) *Lifetime:* Typically, one uses a minimum threshold for the lifetime of tracks (here 3 days are required). A source of error is the cancellation of a track failing this threshold in one set, but not in the other one. This happens frequently if the minimal ages cannot be exactly equal in different temporal resolutions. Since the frequency of tracks depends severely on the minimum lifetime, this is a major source of error.
3) *Distance:* In some studies, a minimum traveling distance is required to eliminate quasi-stationary cyclones, which occur mainly in high spatial resolutions. Another aim could be the elimination of systems caused or trapped by the local orography. This distance threshold is a source of error similar to the minimum lifetime condition, that is, a track may be below the minimum distance in one set, and above in the other set.
4) *Absence of cyclones:* If a high temporal resolution is compared with a low temporal resolution, it is possible that a cyclone is not detected at a time that does not occur in the low resolution. This happens in the initial and the decay phases, when cyclones are weak. The cyclone track is interrupted in the higher resolution and might be canceled due to the minimum lifetime condition. On the other hand, one part of the interrupted track could be identified correctly, the remaining part would be considered to be wrong. The same argument applies to different spatial resolutions, because a cyclone might not be detected at a certain time step in a low spatial resolution.
5) *Wrong attribution:* For large time intervals *dt,* the search areas increase to find the relevant cyclone, but the chance for a wrong detection increases at the same time. This is why larger numbers of tracks are
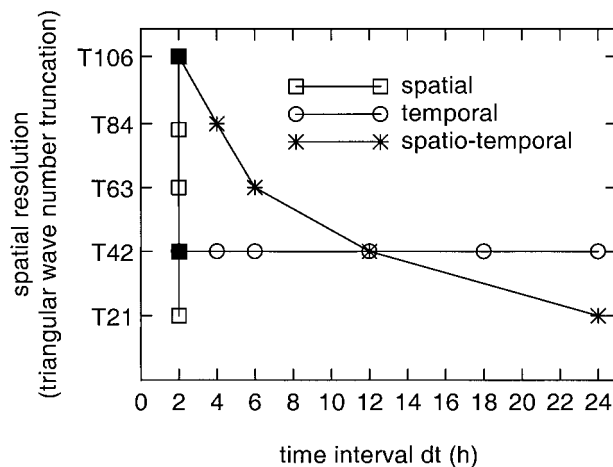
FIG. 2. Overview of the three comparisons: temporal (circles), spatial (squares), and spatiotemporal (stars). The reference resolutions are T42/2 h for the temporal, and T106/2 h for the spatial and the spatiotemporal comparisons.

generated by models with lower temporal resolutions.

5. Results

a. Organization of the comparison

To restrict the analysis to some relevant cases, the following comparisons are performed (see Fig. 2 for an overview).

1) *Temporal:* Tracks obtained in data with increasing time intervals $dt = 4$, 6, 12, 18, and 24 h are compared with $dt = 2$ h reference data (Fig. 2) where the spatial resolution T42 is constant. T42 is chosen because it is sufficient to resolve midlatitude cyclones.
2) *Spatial:* Tracks obtained in the resolutions T21, T42, T63, and T84 are compared with T106 as the reference (Fig. 2); the time interval being $dt = 2$ h. The optimal temporal resolution $dt = 2$ h is chosen to avoid errors due to wrong attributions. The results for $dt = 6$ h are mentioned.
3) *Spatiotemporal:* To investigate the influence of increasing storing capabilities, earlier low resolutions are compared with modern high resolutions. Data in T21/24 h, T42/12 h, T63/6 h, and T84/4 h are compared with T106/2 h as the reference (Fig. 2). This consistent decrease of spatial and temporal scales is also physically relevant.

For each comparison there is a reference track set (set 1), having optimal spatial and temporal resolution, with which the other resolutions are compared (set 2). The number of tracks varies between 100 and 200 and yields reasonable, although not perfect, statistics.

Clearly, these comparisons cannot answer all possible questions on the relations between two resolutions.

However, the results for small differences of resolutions (nearby time intervals and grids) can be estimated by the comparisons presented below.

b. Temporal analysis

To determine the improvement that can be obtained by reducing the time step, a purely temporal analysis is performed. Throughout this part of the study, the spatial resolution T42, since this is sufficient to represent midlatitude cyclones. Datasets with $dt = 2$-, 4-, 6-, 12-, 18-, and 24-h resolution are produced and the cyclone tracks are determined in each dataset. Figure 3 shows the tracks on the Northern Hemisphere for (a) the $dt = 2$ h, and (b) the $dt = 4$ h resolution datasets. The numbers of tracks are (a) 61 and (b) 65 in this region (the complete global dataset is used in the analysis). The tracks in the dataset with $dt = 2$ h are used as reference (set 1) with which all other sets of tracks are compared. The results of the comparison with the $dt \geq 4$ h data are shown in Table 2 (the $dt = 2$ h values are included for orientation).

The number (N_2) of test tracks increases with dt. Therefore, the parameter p_a (7) decreases not only due to lower values N_p of optimal tracks, but also due to higher N_2. The first comparison, $dt = 2$ h with $dt = 4$ h, yields the relatively low value $p_a = 0.94$. A major source for the deviation from $p_a = 1$ is the minimum age condition as discussed above. The probability p_a decays with increasing time interval dt, and for $dt = 24$ h, less than half ($p_a = 0.45$) of the detected tracks can be associated with a track in $dt = 2$ h. The equality of $r_m = 0.12$ for $dt = 6$ h, and $dt = 12$ h is a statistical coincidence. Both ratios p_a and r_m saturate (in the sense that the changes from 18 to 24 h are smaller than those from 12 to 18 h).

The histograms of the distances for the two comparisons 2–4 h and 2–24 h (Fig. 4) show the small distances for the 4-h comparison (a), and a broad distribution for the 24-h comparison (b). However, distances do not vanish in 2–4 h, since the tracks are determined at unequal time steps. The 2–24 h distribution reveals that there is no gap that could be used as a threshold D_c to define associated pairs by $D_{12} < D_c$. This is a reason for the use of optimal pairs in section 4b.

c. Spatial analysis

In this section, the spatial resolutions T21, T42, T63, T84 are compared with T106 and the full temporal resolution of $dt = 2$ h is used. The results are shown in Table 3 together with the mean number N_l of lows (minima in z1000 with an intense gradient g_{min} at each time step. The mean number N_l decreases with the resolution, whereas the ratio p_a of perfect tracks decreases only slightly to 0.75 at T21. The ratio of missing tracks becomes large, $r_m = 0.95$. Briefly, the number of tracks is lower in low resolutions, but most of these tracks are correct. For the larger time step $dt = 6$ h instead of dt
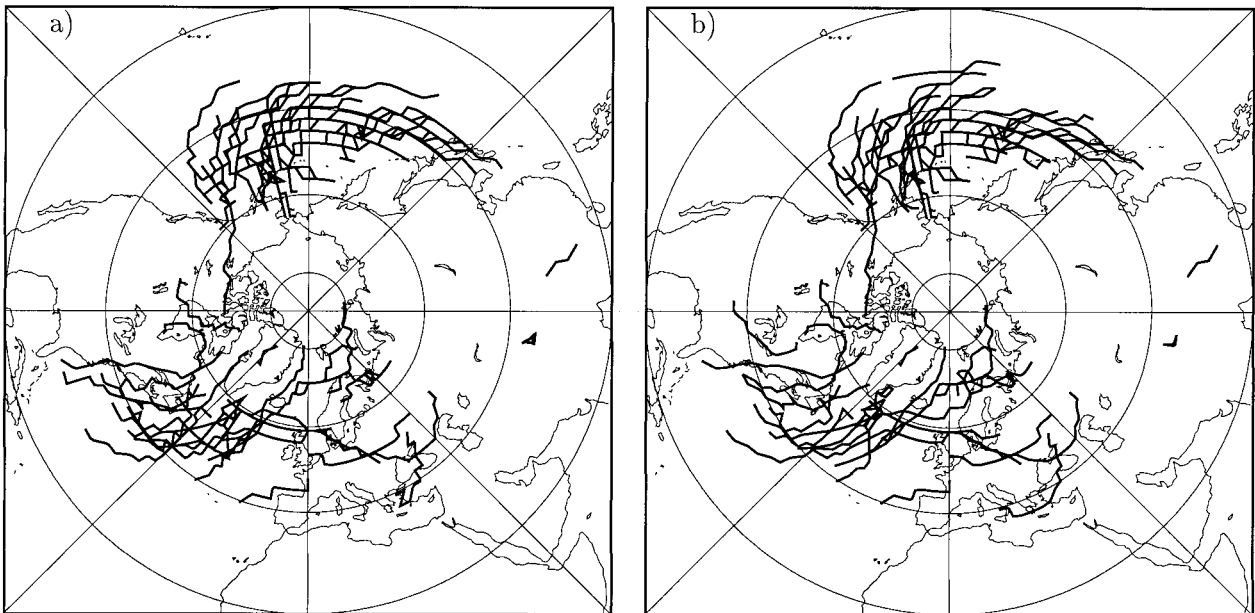
FIG. 3. Cyclone tracks in the Northern Hemisphere determined with temporal resolution (a) $dt = 2$ h and (b) $dt = 4$ h. The spatial resolution is T42, and the numbers of tracks are 61 in (a), and 65 in (b).

= 2 h, the same analysis shows values similar to that in Table 3.

d. Spatiotemporal analysis

Over the course of time, meteorological data have been stored in higher spatial and temporal resolutions synchronously. In this section, the influence of this development is investigated using the series T21/24 h, T42/12 h, T63/6 h, T84/4 h, and T106/2 h, where all data are compared with the latter one. From a physical point of view this series is relevant because it represents a cascade with a simultaneous decrease of spatial and temporal scales. The T106/2 h data is chosen as a reference since only $dt = 2$ h yields reliable tracks.

Table 4 shows the ratio of perfect and missing tracks for this series. The result for T21/24 h is particularly relevant: On one hand, the missing tracks are less frequent than in the pure spatial comparison (Table 3) with $dt = 2$ h, and on the other hand, the ratio of correct tracks is higher than in the temporal comparison (Table 2). This demonstrates that a consistent change of spatial and temporal scales reduces the error.

TABLE 2. Probability p_a for correct tracks and ratio r_m of missing tracks for temporal resolutions $dt \geq 2$ h compared with $dt = 2$ h; the spatial resolution is T42.

dt	2 h	4 h	6 h	12 h	18 h	24 h
p_a	1.00	0.94	0.85	0.73	0.54	0.45
r_m	0.00	0.03	0.12	0.12	0.21	0.26

6. Summary

This study assesses the quality of cyclone tracking in different resolutions. Using a very high–resolution dataset ($1.125° \times 1.125°$, 2 h) produced with the ECHAM4 climate model, data with different spatial and temporal resolutions were derived. Tracks of cyclones, which are defined as minima in the 1000-hPa geopotential height (using an additional intensity condition for the gradient), are determined by a nearest-neighbor search. The search range grows with the time interval according to a power law, which had been observed previously for midlatitude cyclones.

To determine objective measures for the agreement of two sets of tracks, a method is presented that identifies similar tracks in two different sets. The similarity of two tracks is measured by a distance that is based on temporal and spatial variances. The spatial and temporal grids of the two datasets need not be equal. The result describes the expected quality of cyclone tracks detected in test data with given spatial and temporal resolution, when these data are compared with a reference set that has the optimal resolution available in the corresponding study. The method is free of tunable parameters, it is rather general, and can be applied to other problems as well. The results are two ratios, the probability p_a for a track in the test set to be present also in the reference set, and the ratio r_m of tracks missing in the test set but present in the reference set (both ratios are defined with respect to the number of tracks found in the test set).

The study concentrates on main paths in the spatiotemporal diagram (Fig. 2) to answer some of the most relevant questions: What is the influence of a low tem-
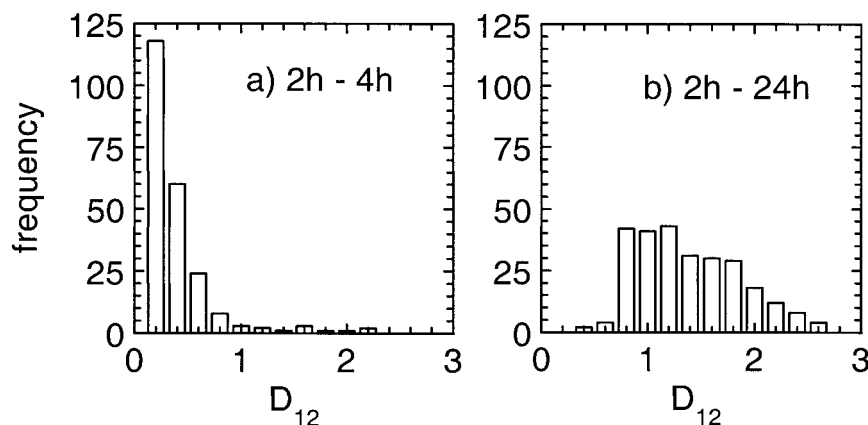
FIG. 4. Frequency of distances D_{12} in the (a) 2–4-h and the (b) 2–24-h comparisons (T42); the bin width is 0.2.

poral or a low spatial resolution, and what happens if both are reduced? Three studies are performed, a first where 2-h tracks are compared with lower temporal resolutions (all at T42), a second comparison of T106 tracks with lower spatial resolutions (time interval 2 h), and a third comparison of T106/2 h tracks with lower spatial and temporal resolutions up to T21/24 h. The main results of the temporal analysis are the satisfactory agreements in 6- and 12-h data ($p_a = 0.85$ and 0.73), and the poor result ($p_a = 0.45$) for the 24-h data. The spatial analysis shows that the majority of the tracks in T21 data are reliable; however, the number of missing tracks is about the same as the number of detected tracks. The spatiotemporal comparison shows that a parallel decrease of spatial and temporal resolution yields a balance with about 50% correct and missing tracks. The number of missing tracks is here lower ($r_m = 0.56$) than in the pure spatial comparison ($r_m = 0.95$) because the increased time interval increases the number of tracks.

7. Discussion

Cyclone paths have been determined since weather maps became available, and the temporal resolution has rarely exceeded 24 h up to the first half of this century. This study shows that the result for cyclone tracks automatically determined in daily data is far beyond the range of acceptable errors. Data with large time steps should be better objectively analyzed using climatological or actual winds to determine a first guess for the

progression of the cyclones, but it is clear that such procedures fail too if the number of cyclones is high, as in high spatial resolutions, for instance. The temporal resolution should be at least $dt = 12$ h, with shorter resolutions still increasing the quality. It is somewhat disappointing that $dt = 4$ h already leads to a considerable discrepancy (94% correct, 3% missing), although one might expect a better agreement. The main reason for this is the minimum age required for cyclone tracks. (This means that a track that lives slightly longer than this threshold in one set can be below the threshold in the second set, which is based on different time grid.)

The method presented yields two numbers, the ratio p_a of perfect, and the ratio r_m of missing tracks, which appear to be reasonable measures when a single test set of tracks is available. Other methods are possible, for example, the use of an averaged distance between the tracks. However, it is difficult to interpret such a distance. Our approach was chosen because it circumvents the definition of a threshold value for the distance: a distance lower (higher) than the threshold would mean agreement (disagreement) of two tracks. An extension of this study would use a longer time series of high-resolution data to improve the statistical reliability of the results. Although the detailed results presented here may depend on the particular tracking method, the overall behavior is certainly reproduceable with other methods. Similar results pertain as well to tracks of other meteorological objects if their density is comparable to the cyclone density.

TABLE 3. Mean number N_l of lows at each time step, probability p_a, and ratio r_m in different spatial resolutions compared to T106; all tracks are determined with 2-h time interval.

Res.	T106	T84	T63	T42	T21
N_l	28.0	23.1	21.7	18.2	13.1
p_a	1.00	0.91	0.88	0.83	0.75
r_m	0.00	0.30	0.32	0.48	0.95

TABLE 4. Probability p_a and ratio r_m of tracks in low spatial and temporal resolutions compared with T106/2 h.

Res./dt	T106/2 h	T84/4 h	T63/6 h	T42/12 h	T21/24 h
p_a	1.00	0.77	0.69	0.65	0.53
r_m	0.00	0.14	0.24	0.31	0.56

REFERENCES

Alpert, P., B. U. Neeman, and Y. Shay-El, 1990: Climatological analysis of Mediterranean cyclones using ECMWF data. *Tellus,* **42A,** 65–77.

Blender, R., K. Fraedrich, and F. Lunkeit, 1997: Identification of cyclone track regimes in the North Atlantic. *Quart. J. Roy. Meteor. Soc.,* **123,** 727–741.

Haak, U., 1993: Variabilität der synoptisch-skaligen Aktivität ausserhalb der Tropen unter klimatologischen Aspekten. Ph.D. dissertation, Universität Köln, 153 pp. [Available from Institut für Meteorologie und Geophysik, Universität zu Köln, Albertus-Magnus-Platz, 50923 Köln, Germany.]

Hodges, K. I., 1994: A general method for tracking analysis and its application to meteorological data. *Mon. Wea. Rev.,* **122,** 2573–2586.

Klein, W., 1957: Principal tracks and mean frequencies of cyclones and anticyclones in the Northern Hemisphere. U.S. Weather Bureau Research Paper No. 40, 60 pp.

König, W., R. Sausen, and F. Sielmann, 1993: Objective identification of cyclones in GCM simulations. *J. Climate,* **6,** 2217–2231.

Murray, R. J., and I. Simmonds, 1991: A numerical scheme for tracking cyclone centres from digital data. Part I: Development and operation of the scheme. *Aust. Meteor. Mag.,* **39,** 155–166.

Roeckner, E., and Coauthors, 1996: The atmospheric general circulation model ECHAM-4: Model description and simulation of present-day climate. Max Planck Institute for Meteorology, Report No. 218, 90 pp. [Available from Max-Planck-Institut für Meteorologie, Bundesstr. 55, D-20146 Hamburg, Germany.]

Schubert, M., 1996: Analyse der Zyklonenzugbahnen über dem Nordatlantik in Kontroll-und Szenarienrechnungen. M.S. thesis, Universität Hamburg, 121 pp. [Available from Meteorologisches Institut, Universität Hamburg, Bundesstr. 55, 20146 Hamburg, Germany.]

——, J. Perlwitz, R. Blender, K. Fraedrich, and F. Lunkeit, 1998: North Atlantic cyclones in CO_2-induced warm climate simulations: Frequency, intensity, and tracks. *Climate Dyn.,* **14,** 827–837.

Sickmöller, M., R. Blender, and K. Fraedrich, 2000: Observed winter cyclone tracks on the Northern Hemisphere in re-analysed ECMWF data. *Quart. J. Roy. Meteor. Soc.,* in press.

Sinclair, M. R., 1997: Objective identification of cyclones and their circulation intensity, and climatology. *Wea. Forecasting,* **12,** 595–612.

Ueno, K., 1993: Inter-annual variability of surface cyclone tracks, atmospheric circulation patterns, and precipitation patterns in winter. *J. Meteor. Soc. Japan,* **71,** 655–671.

Wilshusen, M., 1996: Bestimmung und Auswertung von Zyklonenzugbahnen aus Beobachtungsdaten über dem Nordpazifik. M.S. thesis, Universität Hamburg, 125 pp. [Available from Meteorologisches Institut, Universität Hamburg, Bundesstr. 55, 20146 Hamburg, Germany.]